Materials Science and Engineering C 58 (2016) 790–798

Contents lists available at ScienceDirect

Materials Science and Engineering C

journal homepage: www.elsevier.com/locate/msec

Electrochemical sensing platforms based on the different carbon derivative incorporated interface

Muamer Dervisevic [a], Emre Çevik [a], Zehra Durmuş [b], Mehmet Şenel [c,*]

[a] Department of Genetics and Bioengineering, Faculty of Engineering, Fatih University, B. Cekmece, Istanbul 34500, Turkey
[b] Department of Pharmaceutical Biotechnology, Faculty of Pharmacy, Bezmialem Vakıf University, Fatih, 34093 Istanbul, Turkey
[c] Institute of Biomedical Engineering, Fatih University, B. Cekmece, Istanbul 34500, Turkey

ARTICLE INFO

Article history:
Received 23 June 2015
Received in revised form 2 September 2015
Accepted 10 September 2015
Available online 14 September 2015

Keywords:
Amperometric biosensor
Carbon black
Carbon nanofiber
Extended graphite
Multiwalled carbon nanotube
Reduced graphene oxide

ABSTRACT

In this work we present a comparative study of carbon derivative applications in amperometric biosensors and their effects on the properties of these biosensors. Biosensors were prepared by Horseradish peroxidase (HRP) immobilization on the composite electrodes composed of carbon black, carbon nanofiber (CNF), extended graphite, multiwalled carbon nanotube (MWCNT), reduced graphene oxide (REGO) and poly(glycidyl methacrylate-co-vinylferrocene) (P(GMA-co-VFc)) as mediator, covalent linker, and host matrix for carbon derivatives. The modified pencil graphite electrode (PGE) was used for the detection of hydrogen peroxide and to follow electrochemical behavior of different carbon derivatives which were recorded. The electrochemical characterization was investigated by cyclic voltammetry and electrochemical impedance spectroscopy methods. Amperometric measurements showed that the REGO and MWCNT modified electrodes have excellent performance in comparison with other carbon derivatives studied.

1. Introduction

Biosensors are generally defined as analytical devices — or units incorporating a biological or biologically derived sensing element, integrated or associated with a physio-chemical transducer [1–3] which converts a biological response into a quantifiable and processable signal [4,5]. Whereby biosensor is composed of three main parts: (1) the biological recognition element that recognizes the target molecule in the presence of various chemicals, (2) a transducer which converts the bio-recognition event into a measurable signal, and (3) a signal processing system that converts the signal into readable form [3,6–8]. Biosensors have two basic principles which differentiate them from chemical sensors: (i) sensing elements, which are biological structures such as cells, enzymes, or nucleic acids, and (ii) the sensor's usage for measurements of biological processes or physical changes [9]. Owing to the constant desire for developing a biosensor which fulfills the contemporary necessities at the time of unceasing technological development, we can produce small compact devices of higher sensitivity, greater analytic determination, and lower operating costs.

Nowadays, there are different methods used to detect biological and environmental chemicals, including high performance liquid chromatography (HPLC) [10,11], gas chromatography [12], chemiluminescence [13], and spectrophotometry [14]. Biosensors especially based on electrochemical methods are mostly used and have increasing trend to the analysis of biological and environmental substances. Due to the onsite detection, low cost, fast response, high sensitivity, simple instrumentation, and low energy requirement electrochemical techniques for determination of these substances have been studied. [15–19].

Amperometric biosensors are one of the most studied sensor types because of their real-sample application ability, high sensitivity, wide range of analyte detection, and lower operating costs. One of the studied amperometric biosensors is based on Horseradish peroxidase (HRP) for hydrogen peroxide (H_2O_2) detection [25] being a byproduct of several highly selective oxidases and also an essential mediator in food, biology, industry, environmental analysis, and medicine [20,21,26]. H_2O_2 is also characterized as non-radical reactive oxygen species (ROS), and ROS is accounted as one of the responsible species for mutagenic DNA damage in mammalian cells [22]. Many techniques for H_2O_2 determination have been employed such as spectroscopy [23], chemiluminescence [24], and titrimetry [25]. Because these techniques have some drawbacks such as interferences, long analysis time, and involvement of expensive reagents, they hardly fit into technological demands that continuously expand. One of the ways of achieving good electron transfer ability in amperometric biosensors is to introduce a mediator such as ferrocene between enzyme and electrode. Ferrocene (Fc) polymeric mediators are widely used to construct mediated amperometric biosensors due to the properties of having excellent electron transfer capability and allowing the incorporation of reagents to the sensing system that may be a requirement for further sensor developments [25]. Some redox copolymers widely used

* Corresponding author.
E-mail address: msenel@fatih.edu.tr (M. Şenel).

http://dx.doi.org/10.1016/j.msec.2015.09.052
0928-4931/

for the covalent attachment of ferrocene are ferrocene-containing polythiophene derivatives [27], poly(vinylferrocene-co-hydroxyethyl methacrylate) [18], acryl amide copolymers [29], poly(glycidyl methacrylate-co-vinylferrocene) [16], and poly(N-acryloylpyrrolidine-co-vinylferrocene) [30]. The electrochemical behavior of Fc (Fc → Fc+) attributed to the redox couple has been proved to be highly effective for electrode modification and functionalization [31]. Various ferrocene bioelectrodes have been developed to show the effectiveness of Fc derivatives such as in the study reported by Şenel et al. [36] named "amperometric hydrogen peroxide biosensor based on covalent immobilization of horseradish peroxidase on ferrocene containing polymeric mediator", another research has been reported by the Erden et al. [32] named "amperometric enzyme electrode for xanthine determination with 1,4 benzoquinone and poly (vinylferrocene) as a mediators", and by Tanushree et al. [31] in which uric acid biosensor is developed based on uricase electro-activated with ferrocene on a Nafion coated glassy carbon electrode. In general, construction of biosensor has to be designed with the emphasis on tight fixation of the mediator (and all other sensor components needed) to the electrode surface to create so-called "reagentless" biosensors [33].

Nanomaterials, particularly carbon based nanomaterials, have been the subject of intense research over the past twenty years [34,35], and they have a significant role to play in new developments in each of the biosensor size domains as they can help address some of the key issues in the development of all biosensors [36,37]. Those main issues include: i) constructing and developing of the biosensing interface so that the analyte can easily interacts with the biosensing surface [38,39]; ii) achievement of efficient transduction of the biorecognition event [36,40,41]; iii) increment in the sensitivity and selectivity of the biosensor [42,43]; and iv) improvement of response time in very sensitive systems [44]. There has been an explosion of interest in application of nanomaterials such as carbon black (C.Black), carbon nanotubes (CNTs), carbon nanofiber (CNF), expanded graphite (E.Graphite), and reduced expanded graphite oxide—(it is called as graphene in the text) (REGO) for the development of amperometric biosensors. Carbon derivative important properties and application in amperometric biosensor selected examples have been summarized in Table 1.

In this work, we aim to determine the performance effect of the carbon derivatives on amperometric detection that is important for the consistency of the sensor's system fabrication. Although almost all of the carbon derivatives were studied for biosensor development to obtain highly efficient amperometric biosensors, these studies were not effectively conducted together under the same experimental setup. For the purpose of obtaining good electrochemical signals the hydrogen peroxide biosensor was constructed as model biosensor. This study indicates that REGO and MWCNT have an important role in terms of providing enhanced electrochemical sensing properties to biosensors when compared with other carbon materials studied.

2. Experimental part

2.1. Materials

Horseradish peroxidase (HRP) was purchased from Sigma-Aldrich (USA), vinylferrocene (VFc) purchased from Aldrich (Japan) and Glycidyl methacrylate and hydrochloric acid (37% HCl) were purchased from Sigma-Aldrich (Germany), Iron (III) nitrate nonahydrate, $Fe(NO_3)_3 \cdot 9H_2O$, iron (II) chloride tetra hydrate ($FeCl_2 \cdot 4H_2O$), sulfuric acid (H_2SO_4 fuming), hydrogen peroxide (30% H_2O_2), potassium permanganate ($KMnO_4$), ammonia solution (28% NH_3), sodium nitrate ($NaNO_3$), and hydrazine hydrate ($N_2H_4 \cdot H_2O$) were purchased from Merck (Germany). All the chemicals employed in the study were analytical grade and used as-received without purification. The EG was a commercial grade, thermally expanded product (TIMREX® BNB90), kindly provided by TIMCAL (Switzerland). The density, surface area, average particle size (d_{90}) and the oil adsorption number (OAN) values of EG were reported as 2.24 g/cm^3, 28 m^2/g, 85.2 μm and 150 ml/100 mg, respectively by the producer.

2.2. Preparation of poly (GMA-co-VFc)

The redox polymer, containing different compositions, was prepared according to our previous study [91]. A mixture of vinylferrocene (VFc) and glycidyl methacrylate (GMA) at a known molar ratio was injected into a Pyrex tube, AIBN (1 mol% based on the total monomer concentration was identical for all samples, 5 mol/dm^3), after which the mixture was degassed with Argon gas and vacuum sealed. In the next step, the tubes were placed in constant temperature baths, with constant temperature of 70 °C for 2 days. After, the reaction mixture was added drop wise, while rapidly stirring the diethyl ether to precipitate the copolymer. In the end, precipitated copolymer was washed with diethyl ether and reprecipitated in this manner, twice and finally vacuum dried.

Table 1
Comparison of different carbon derivatives properties and applications in different amperometric biosensors.

Carbon derivatives	Properties	Biosensor application
C.Black	–particles with diameter ranging from 15 to 100 nm [45], hard to disperse and easy to flocculate [46] –hard to disperse and easy to flocculate and strong cohesion between particles [46] –many polar radicals from the surface of particles and has large specific surface area in form of its congeries [46] –not widely used in biosensor applications [46].	Laccase [45] Glucose [46] Nerve agents [48] Bisphenol A [95]
E.Graphite	–widely used as gasket, fire resistant composite, thermal insulator [49–51], –has an important degree of crystallinity, long-range disorder, and high degree of porosity [52] –high compressibility and elastic recovery, chemical resistance and good thermal and electrical conductivity [52] –lamellar structure of graphite and can exhibit high porosity up to 99% [49] –good dispersion in a polymer matrix. [53]	Urea [55] Nitrate and nitrite [56] Phenol [57]
REGO	–high crystal quality and quite unusual electronic properties [59], excellent conductor [60] –enhanced electrochemically active site [62,63], and good biocompatibility –large number of electroactive sites in big area of its structure [61], high surface to volume ratio –excellent thermal conductivity, mechanical flexibility, chemical tolerance	H_2O_2 [69,67] Proteins [68] Pesticides [100] Glucose [70]
CNF	–submicron diameter sizes (typically below 100 nm) [71], they have been used as catalyst and catalyst support [75] –mechanical and thermal properties, high tensile strength and elastic modulus [74,75] –contain more edge sites on the outer wall [74], high electric conductivity [73] –they can facilitate the electron transfer of electroactive analytes [77], larger functionalized surface area [78] –one-dimensional macrostructures [81,72]	Dopamine and serotonin [79] H_2O_2 [80] Acetylcholine [101]
MWCNT	–have huge impact on amperometric biosensors due to the ability to blend into a number of formulations in order to improve current densities and overall performance of enzyme electrodes [82,83]. –huge importance for the production of renewable energy and construction of electrochemical sensors [83,86] –subtle structural changes that switch tubes from metallic to semiconducting having various band gaps [87] –electron transfer reaction with wide range biosensor applications [88] –incorporation of carbon nanotubes leads to fast electron transfer, lower limit detection, and high sensitivity [89]	H_2O_2 [90,84] Xanthine [96] Pesticides [98] Dopamine [99] Urea [97]

2.3. Synthesis of REGO

In the first step, EG was oxidized by the well-known modified Hummers [92] method to prepare EGO. In the second step, EGO powder was dispersed in the deionized water in a flask and a stable yellow-brown dispersion was obtained due to the hydrophilic nature of EGO. Hydrazine monohydrate which is the most frequently used reducing agent due to the simplicity of its application procedure and the reduction efficiency to obtain graphene sheet having excellent physical properties [93], was then added to the EGO suspension. The flask equipped with a water-cooled condenser was heated up to 100 °C in an oil bath and kept at this temperature for 24 h. The EGO sheets were reduced to form graphene nanosheets or reduced expanded graphite oxide, REGO, and gradually precipitated out as a black solid due to the hydrophobic nature of REGO sheets. The REGO was isolated by filtration and washed with the excess of water and methanol then dried in a vacuum oven.

2.4. Preparation of enzyme electrode

Pencil graphite electrode (PGE) fabrication was initiated by rinsing meticulously the 2 to 10 mm area from the tip of the electrode with acetone followed by distilled water (DW). Composites including different carbon derivatives (CNT, CNF, REGO, C.Black, E.Graphite) were prepared by mixing with P(GMA-co-VFc) in ratio of 2.5 mg/ml separately (Fig. 1). After DW drops completely dried 5 μL portions of each composite were carefully spread over the different electrode surfaces. All the electrodes

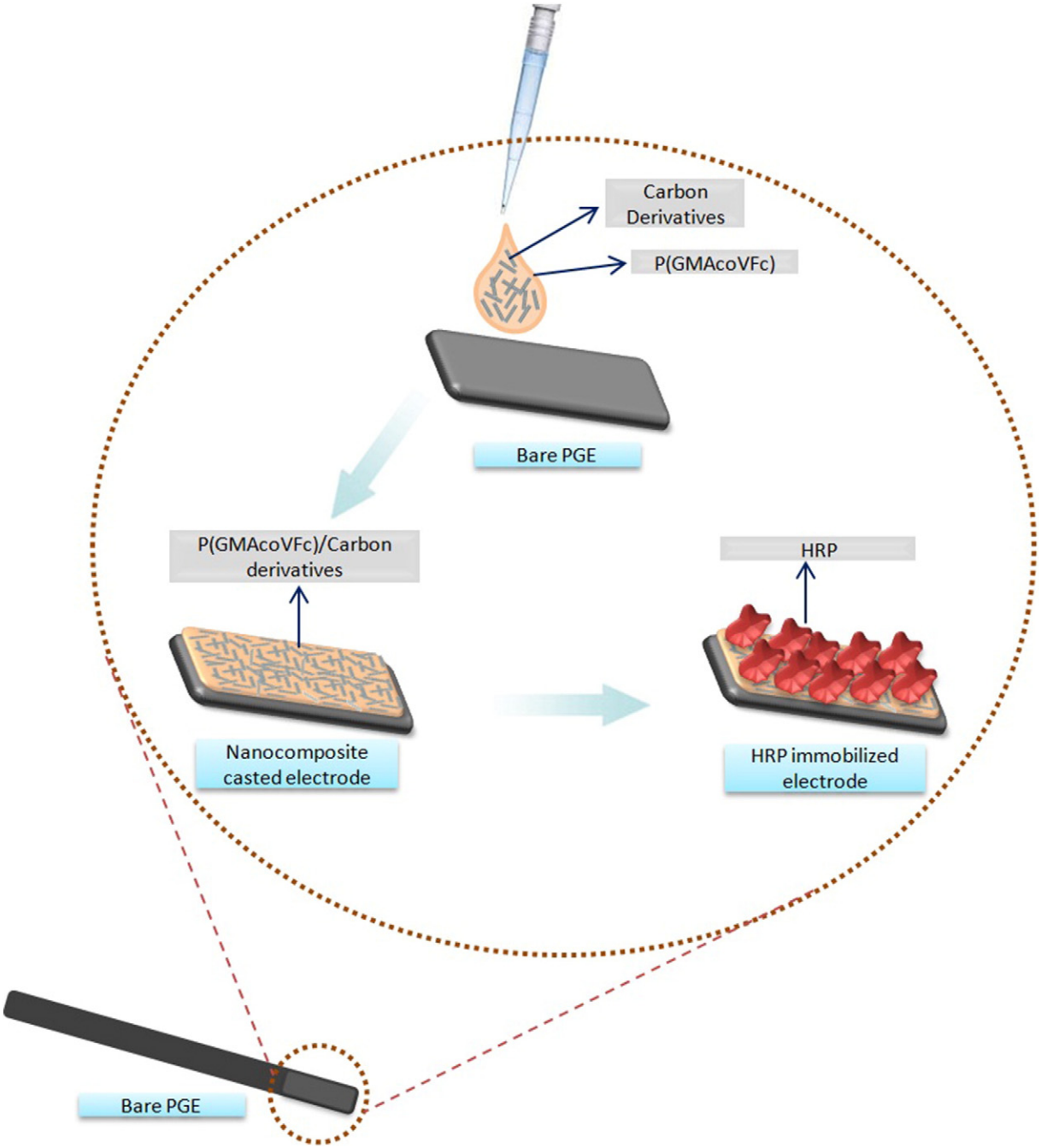

Fig. 1. The schematic illustration of fabrication process of the biosensor.

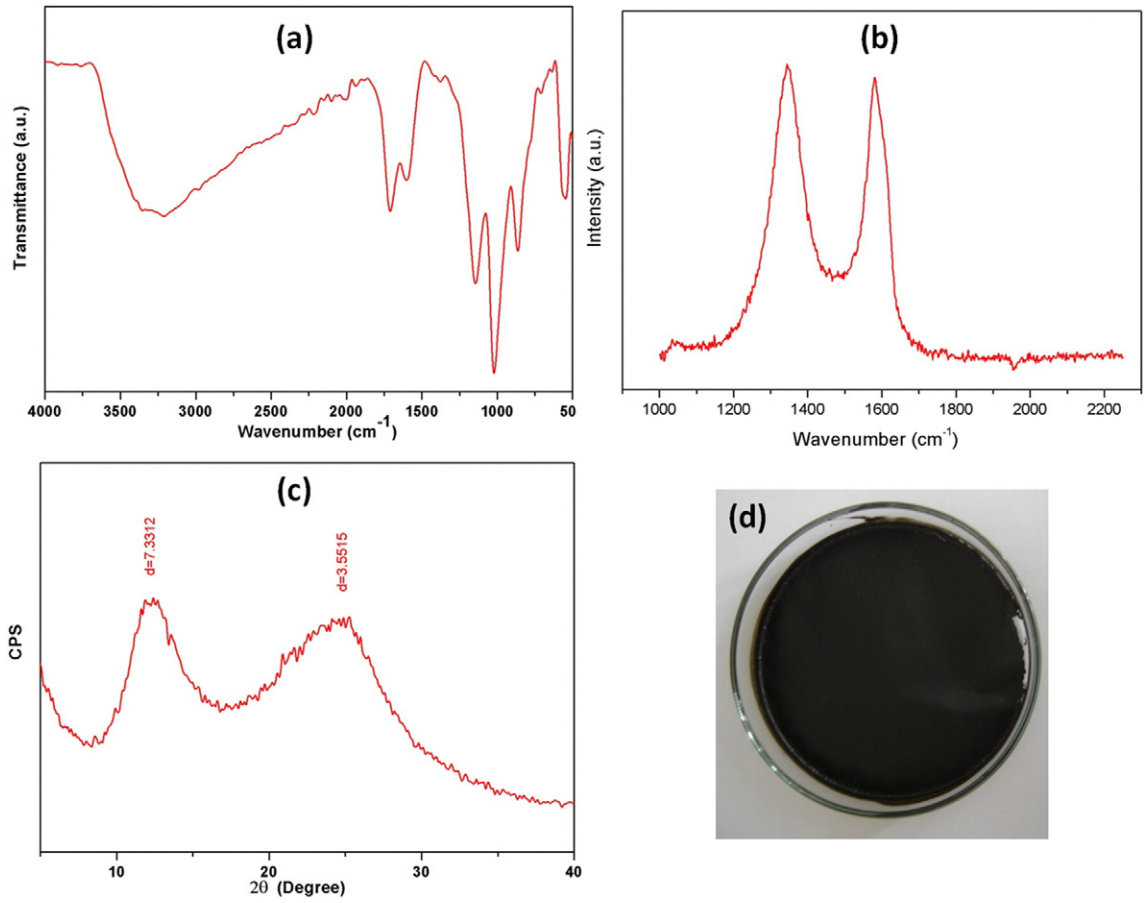

Fig. 2. a) FT-IR spectrum, b) Raman spectrum, c)XRD pattern and d) photograph of synthesized reduced expanded graphite oxide-REGO.

were placed in drying-oven set at 60 °C for a faster surface drying process and kept until the polymer was sufficiently adsorbed. Subsequently, it was first rinsed with 10 mM PBS at a pH of 7.0 after, it was immersed in 5 mg/ml of HRP dissolved in PBS (pH 7.0) then it was placed on an orbital shaker adjusted to 120 rpm and placed at 4 °C, for 48 h. The working electrode was washed carefully with a few drops of PBS (pH 7.0) prior to using and stored in PBS (pH 7.0, 0.1 mM) at 4 °C while not used.

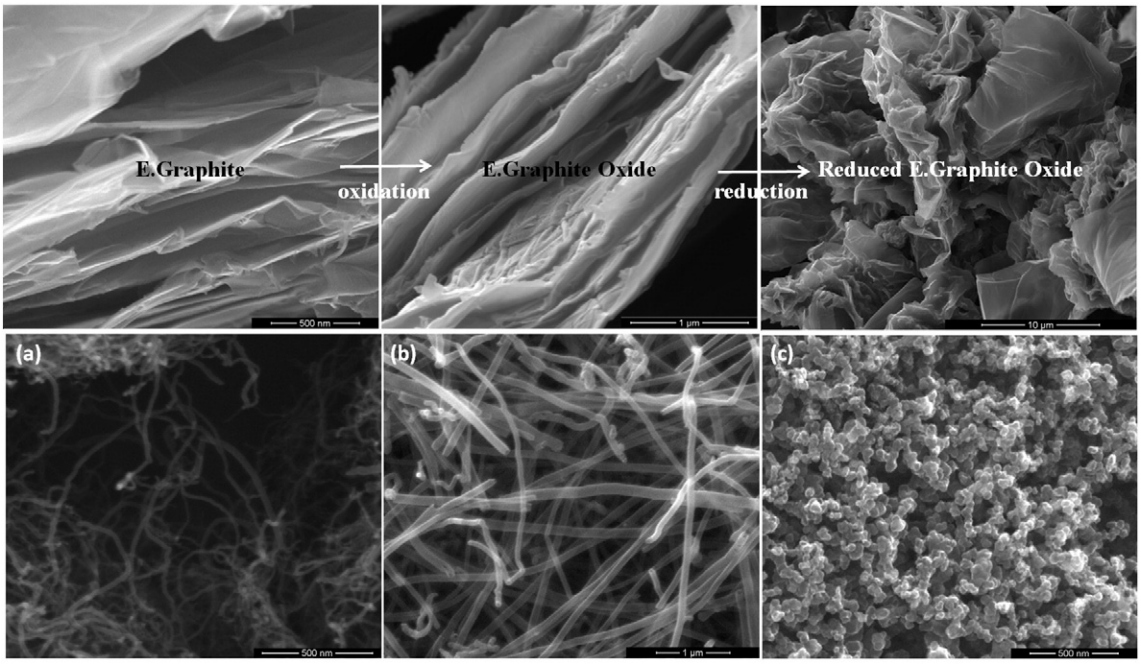

Fig. 3. SEM micrographs of E.Graphite, E.Graphite oxide, Reduced E.Graphite oxide (a) MCNT, (b) CNF, and (c) C.Black.

2.5. Instrumentations

The XRD patterns of samples were obtained by using a Rigaku Smart Lab XRD with Cu-K_α radiation at room temperature. FTIR spectra were recorded in transmission mode with a Bruker Alpha infrared spectrometer using the ATR mode, in the range of 400–4000 cm^{-1} with the resolution of 2 cm^{-1}. The Raman spectra of graphitic materials were also recorded in a Thermo-Fisher Scientific, DXR dispersive Raman instrument using laser excitation of 532 and 780 nm and an InGaAs detector, in the range of 400–3500 cm^{-1}. One hundred scans were accumulated with the resolution of 4 cm^{-1} by using a laser power of 100 mW.

Electrochemical measurements were performed using CompactSoft portable electrochemical interface and impedance analyzer (*Ivium Technologies*). The electrochemical measurements were recorded via a three electrode system which was composed of Ag/AgCl as reference, Platinum wire as auxiliary, and PGE/P(GMA-co-VFc)/(CNT, CNF, REGO, C.Black, E.Graphite) as working electrodes all immersed in an electrochemical cell filled with 10 mM PBS (pH = 7.4) and applied potential of +0.35 V. Conventional three-electrode electrochemical cell was purchased from CH Instruments. After allowing the steady-state current to be reached, the HRP catalysis was triggered by H_2O_2 additions to the buffer solution from working cell being continuously stirred at room temperature.

Electrochemical impedance spectroscopy (EIS) measurements were carried out using a CHI Model 6005 electrochemical analyzer in a background solution of 5 mM Fe^{3+}/Fe^{2+} phosphate buffer (pH 7.4). The alternating voltage was 5 mV and the frequency range was 5.0×10^{-2} to 1.0×10^{6} Hz.

Two scanning electron microscope (SEM) was employed to observe the surface of the samples. For SEM, pieces of the membranes were mounted on stubs and coated with gold using a sputter coater. SEM micrographs of the samples were taken using a field emission SEM (FESEM, FEI Quanta FEG 450) and a JEOL NeoScope scanning electron microscope operated at 30 kV.

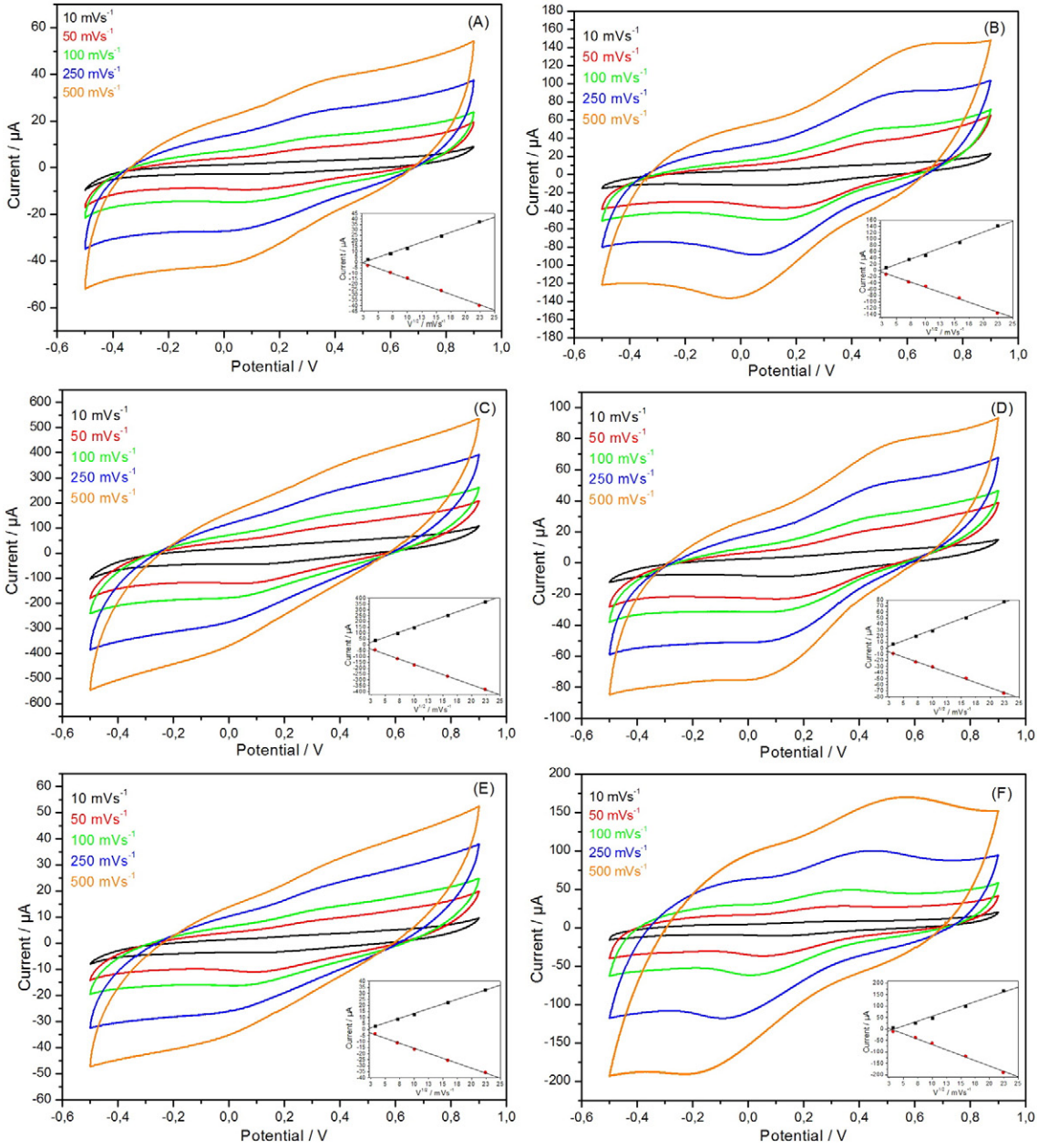

Fig. 4. Cyclic voltammogram of A) P(GMA-co-VFc), B) P(GMA-co-VFc)/C.Black, C) P(GMA-co-VF)/REGO, D) P(GMA-co-VFc)/E.Graphite, E) P(GMA-co-VFc)/CNF, F) P(GMA-co-VFc)/MCNT coated electrodes with different scan rates in 10 mM PBS solution, pH 7.4.

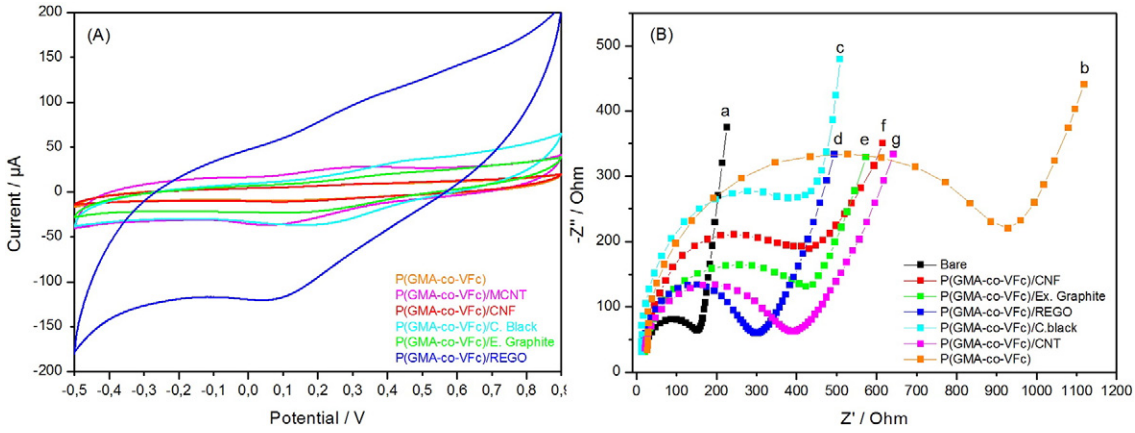

Fig. 5. A) Cyclic voltammogram of a) bare electrode, b) P(GMA-co-VFc), c) P(GMA-co-VFc)/C.Black, d) P(GMA-co-VF)/REGO, e) P(GMA-co-VFc)/E.Graphite, f) P(GMA-co-VFc)/CNF, and g) P(GMA-co-VFc)/MCNT, coated electrodes in 10 mM PBS solution, pH 7.4. B) Electrochemical impedance spectra of a) bare electrode, b) P(GMA-co-VFc), c) P(GMA-co-VFc)/C.Black, d) P(GMA-co-VF)/REGO, e) P(GMA-co-VFc)/E.Graphite, f) P(GMA-co-VFc)/CNF, and g) P(GMA-co-VFc)/MCNT, coated electrodes in 10 mM PBS solution, pH 7.4.

3. Results and discussion

3.1. Materials characterizations

FTIR, and RAMAN spectrum and XRD patterns of the EG, EGO and REGO employed in this study were given in Fig. 2 and also previously reported [94].

Fig. 3 shows SEM micrographs of EG, EGO, and REGO respectively. In Fig. 3, highly porous and layered structure of commercial EG having large stacks, possibly consisting of hundreds of graphene nanosheets, can be clearly seen. Post-oxidation, the SEM micrograph shows of the oxidized counterpart, EGO. The mean size of graphitic nanosheets was not disrupted with the oxidation, but the surface properties of modified product were strongly affected. As seen in Fig. 3, the surfaces of EGO nanosheets are rough, and the edges are highly crumpled. On the other hand, after strong reduction the SEM image REGO clearly signifies the very thin, wrinkled, loose open and transparent graphene sheets obtained by the chemical reduction process [94]. In Fig. 3A SEM micrograph of CNTs indicates their tubular 1D morphologies with a network structure. In addition, fiber frame of CNFs and spherical 3D build of carbon black have seen clearly in Fig. 3.

3.2. Electrochemical characterizations

To investigate and characterize electrochemically active different electrode systems, cyclic voltammetry (CV) method was used and voltammograms were recorded. Because of the characteristic plot of P(GMA-co-VFc) voltammogram the number of oxidation states and electron transfer rates of the carbon derivatives were monitored according to changing of peak currents (Ipa and Ipc). This was achieved by the different semi conductor properties that carbon materials have. Initially, different carbon derivatives were fabricated on pencil graphite electrodes as a film and electrochemical properties were measured by cyclic voltammetry (shown in Fig. 4A-f). The effect of scan rate on the peak current (Ipa and Ipc) were obtained and results are recorded between scan rate of 10 mV s^{-1} and 500 mV s^{-1} in 100 mM pH 7.4 PBS. Fig. 4A shows the typical redox couple of P(GMA-co-VFc) electrode at the different scan rates in the potential ranging from −0.5 to 0.9 V. Anodic peak potential (Epa) was recorded at value of 0.35 V which is related to oxidation of polymer and the cathodic peak potential (Epc) obtained at 0.15 V is attributed to its reverse process. A quasi reversible electrochemical process can be observed that as the scan rate increases peak currents and the difference between the peak potentials are increased. The plot of peak currents (Ipa and Ipc) and square root of scan rate ($v^{1/2}$) inset to Fig. 4A showing that a linear relation. This linearity between peak currents and scan rate, indicates the diffusion controlled redox process during the forward scan (in which (Fe(II) is oxidized to Fe(III)) and reverse scan (in which Fe(III) is reduced) at the P(GMA-co-VFc) modified electrode. The rest of the cyclic voltammograms shows that the relationship between peak currents and the scan rates of different composites made of carbon-based materials such as C.Black, REGO, E.Graphite, CNF and MWCNT are mixed with P(GMA-co-VFc). As seen in the figure, any specific redox peaks of the materials were observed. However, it was found that each carbon derivative increases the difference between the reduction and oxidation peaks of the polymer. Fig. 4D reveals that P(GMA-co-P(GMA-co-VFc)/E.Graphite modified electrode exhibited almost two times higher peak current when compared to the P(GMA-co-VFc) modified electrode. On the other hand well observed redox peaks were exhibited from (Fig. 4B and f) P(GMA-co-VFc)/C.Black and P(GMA-co-VFc)/MCNT coated electrodes almost four times higher peak current. The maximum plot of peak current (ten times higher) was obtained from P(GMA-co-VF)/REGO modified electrode with respect to the scan rate (Fig. 4C). Considering the peak currents (Ipa and Ipc), each of the composites has positively enhanced electron transfer rate of redox couples. However potentials of anodic and cathodic peaks were slightly shifted towards more positive and more negative sites, which could be attributed to the limitation of electron diffusion rate. This limiting effect can be explained by the effect of carbon derivative interaction with polymer. The increasing behavior of peak current with increasing scan rate are true for all different carbon electrodes. Also the linear correlation between peak current and square root of scan rate is increased with increasing scan rate predicted that for all composites, a well controlled redox process occurred by controlling the ion diffusion, changing of oxidation and reduction.

Fig. 5A shows the cyclic voltammogram of different carbon-based material coated pencil graphite electrode at a constant scan rate of 10 mV s^{-1} between −0.5 and 0.9 V in 100 mM PBS. The characteristic quasi-reversible peaks of the redox couples at the P(GMA-co-VFc), P(GMA-co-VFc)/C.Black, P(GMA-co-VF)/REGO, P(GMA-co-VFc)/E.Graphite, P(GMA-co-VFc)/CNF, P(GMA-co-VFc)/MCNT electrodes were

Table 2
R_{ct} values of modified electrodes with different carbon derivatives.

Electrode	R_{ct} (Ω)
PGE	150
p(GMA-co-VFc)	850
p(GMA-co-VFc)/CNT	380
p(GMA-co-VFc)/CNF	435
p(GMA-co-VFc)/C. Black	410
p(GMA-co-VFc)/E. Graphite	430
p(GMA-co-VFc)/REGO	290

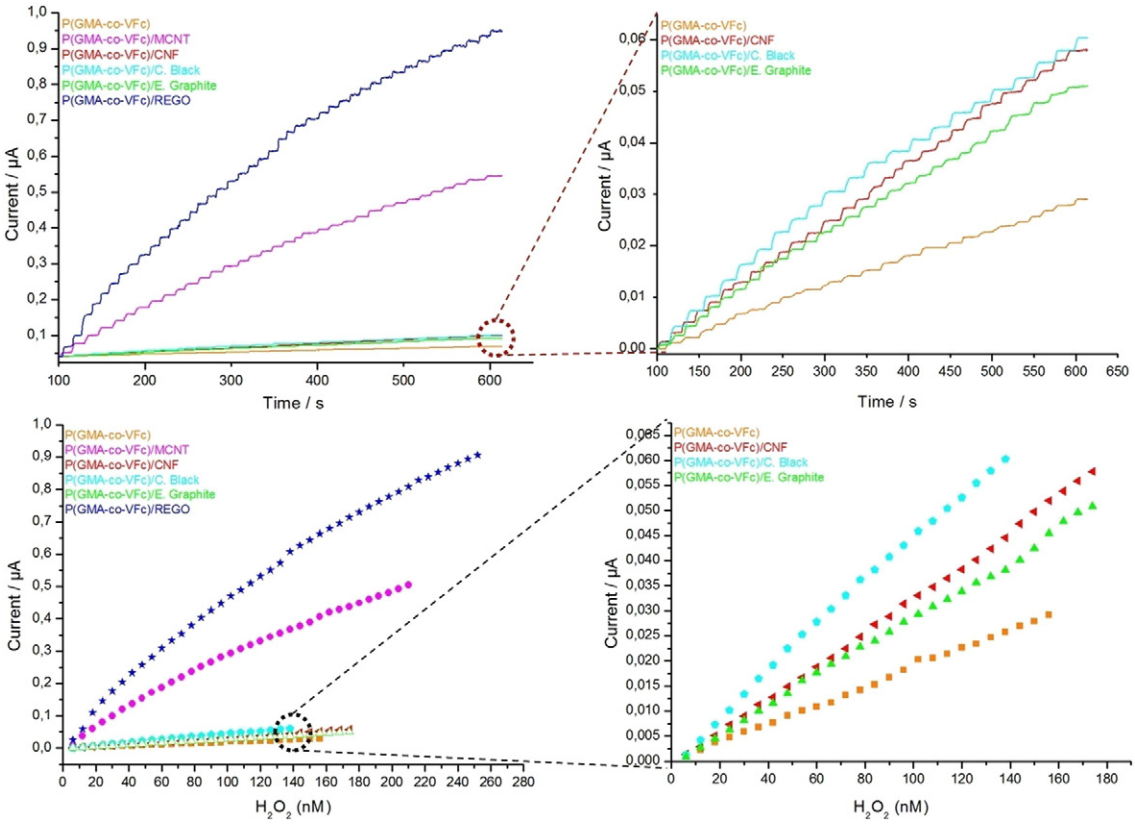

Fig. 6. A typical amperometric response current plots and calibration curves of different HRP immobilized electrodes to successive addition of 6 nM hydrogen peroxide at an applied potential +0.35 V in stirred 10 mM PBS (pH 7.4; ~25 °C).

shown with peak current differences ΔI = 18.4, 18.9, 42, 64, 67, and 210 μA respectively. The greater ΔI was recoded from the REGO modified electrode. This is proved by recording a small R_{et} value as plotted in Fig. 5B which exhibited improved electron and mass transfer because of the increased surface area provided by the extended two dimensional structure of REGO. Furthermore this result reveals that well incorporated particles with the polymer accelerate electron transfer rate due to uniform dispersion. However the CNF modified electrode gave almost the same CV curve with the polymer. This can be explained either polymer or CNF are not well integrated to each other and this caused to gaps formation or the density of the CNF limits the electron diffusion.

Fig. 5B shows the Nyquist plots of the electrochemical Impedance spectra for P(GMA-co-VF) with different carbon-based composites modified pencil graphite electrode. The diameter of the semicircular part represents electron transfer resistance R_{ct} at high frequencies and linear part which is related to diffusion control at lower frequencies. At "high" frequency, the impedance demonstrates infinite diffusion behavior (phase angle 45°) while at "low" frequency, it tends to show the capacitor behavior (phase angle 90°) [67]. The electron transfer resistance at the surface of PGE modified electrode can be assessed by evaluating semicircle diameter, as shown in Table 2. R_{ct} values for modified electrodes are as follows:

Here the R_{ct} values are decreased starting from p(GMA-co-VFc) which has a value of 850 Ω, to the minimum value 290 Ω which was obtained from REGO (Fig. 5B). The bare electrode shows a line with a very small semicircle diameter due to the subsistent conductivity of bare pencil graphite electrode. The higher R_{ct} value of polymer implies that it acts as insulating layer which caused interfacial charge transfer that is very weak as compared with bare electrode. Among the carbon derivatives R_{ct} value of 290 Ω with smaller diameter was obtained from p(GMA-co-VFc)/REGOs, suggesting better electron transfer efficiency. It also indicates the successful formation of the films and well particle distribution affects the charge transfer on the electrode surfaces. In the end, different carbon derivatives have electron efficiency in order from maximum REGO-CNT-C.Black-E.Graphite-CNF and p(GMA-co-VFc) to minimum efficiency. However study showed that carbon derivatives in between (CNT-C.Black-E.Graphite-CNF) had relatively close R_{ct} value. Finally, electron transfer efficiency of all the carbon derivatives appears to be higher than polymer. However, if the comparison is made between them, the REGO is higher although results are close together. This shows that the R_{ct} value depends on conductivity of the materials, particle size and distribution.

Table 3
Comparison of analytical performance of carbon derivatives in biosensor.

Electrode	DL (nM)	Sensitivity (nA/mM)	LR (nM)	RT (s)	R^2
p(GMA-co-VFc)	0.660	1.29	6–156	8	0.9982
p(GMA-co-VFc)/MCNT	0.340	16.71	6–108	3	0.9937
p(GMA-co-VFc)/CNF	0.051	2.19	6–174	4	0.9992
p(GMA-co-VFc)/C. Black	0.003	2.83	6–138	5	0.9987
p(GMA-co-VFc)/E. Graphite	0.051	1.73	6–174	4	0.9979
p(GMA-co-VFc)/REGO	0.020	27.44	6–102	2	0.9959

DL, detection limit; LR, linear range; RT, response time.

3.3. Amperometric response of biocomposite electrode

In this work, different carbon derivative based composites were used to modify electrode and the analytical performances of the biosensor were compared. Under the optimized conditions the amperometric response of the biosensors was examined by successive addition of hydrogen peroxide solution in a continuously stirred PBS (10 mM PBS pH 7.4). Fig. 6 shows the typical current vs time plots of the prepared biosensors and the current increased with the addition of H_2O_2. The analytical performances of the prepared biosensors were compared with

each other as shown in Table 3. The change in the electrochemical signal (Δi) obtained in the presence of REGO was clearly much larger than the other carbon derivatives, and the linear relationship was excellent. The sensitivity and the detection limit of the REGO were 27.44 nA/mM and 0.020 nM, respectively, (S/N = 3). The prepared REGO modified biosensor showed high sensitivity, low detection limit, and fast response, which could be attributed to good electrocatalytic activity and high conductivity. Also, the MWCNT based biosensing electrode showed good amperometric response. This behavior could attribute to the REGO and MWCNT on the electrode surface, which endowed the good electrical conductivity and then efficiently accelerated the electron transfer than others as also shown in CV and EIS results. Moreover, the incorporation of the REGO and MWCNT has greatly improved the sensitivity of the biosensor compared with the others as seen in Table 3.

4. Conclusions

In this work, electrochemical performance of the different carbon derivatives was studied in one biosensor construction to make the inclusive evaluation. The hydrogen peroxide biosensor was constructed as a model biosensor by using P(GMA-co-VFc) as mediator and covalent linker for immobilization of HRP due to its ferrocene and epoxy functionalizations. The CV and EIS results demonstrated that REGO and MWCNT are the most efficient carbon derivatives for the electrochemical amperometric biosensor electrode construction. The amperometric biosensing results under the same experimental conditions also clearly indicated that REGO and MWCNT based electrochemical biosensors could greatly improve the performance of amperometric detection.

References

[1] A.P. Turner, Biosensors—sense and sensitivity, Science 290 (2000) 1315–1317.
[2] L. Song, G. Xuefeng, Carbon nanomaterials field-effect-transistor-based biosensors, NPG, Asia Mater. 4 (2012) 1–10.
[3] Y. Eun-Hyung, L. Soo-Youn, Glucose biosensors: an overview of use in clinical practice, Sensors 10 (2010) 4558–4576.
[4] C.R. Lowe, Biosens. Tren. Biotechnol. 2 (1984) 59–65.
[5] G. Dorothee, M. Robert, V. Janos, R. Erik, Electrochem. Biosens. Sens. 8 (2008) 1400–1458.
[6] L.C. Clark, C. Lyons Jr., Electrode systems for continuous monitoring in cardiovascular surgery, Ann. N.Y. Acad. Sci. 102 (1962) 29–45.
[7] S.J. Updike, G.P. Hicks, The enzyme electrode, Natu. 214 (1967) 986–988.
[8] A. Hiratsuka, K. Fujisawa, H. Muguruma, Amperometric biosensor based on glucose dehydrogenase and plasma-polymerized thin films, Anal. Sci. 24 (2008) 483–486.
[9] L. Yuanyuang, J.S. Hermann, X. Shunqing, Gold nanoparticle-based biosensors, Gol. Bulle. 43 (2010) 29–41.
[10] V. Carrera, E. Sabater, E. Vilanova, M.A. Sogorb, A simple and rapid HPLC–MS method for the simultaneous determination of epinephrine, norepinephrine, dopamine and 5-hydroxytryptamine: application to the secretion of bovine chromaffin cell cultures, J. Chromatogr. B 847 (2007) 88–94.
[11] E.C. Chan, P.Y. Wee, P.Y. Ho, P.C. Ho, High-performance liquid chromatographic assay for catecholamines and metanephrines using fluorimetric detection with pre-column 9-fluorenylmethyloxycarbonyl chloride derivatization, J. Chromatogr. B 749 (2000) 179–189.
[12] D.L. Kuhlenbeck, T.P. O'Neill, C.E. Mack, S.H. Hoke II, K.R. Wehmeyer, Determination of norepinephrine in small volume plasma samples by stable-isotope dilution gas chromatography–tandem mass spectrometry with negative ion chemical ionization, J. Chromatogr. B 738 (2000) 319–330.
[13] Z. Lin, X. Wu, X. Lin, Z. Xie, End-column chemiluminescence detection for pressurized capillary electrochromatographic analysis of norepinephrine and epinephrine, J. Chromatogr. A 1170 (2007) 118–121.
[14] M. Zhu, X.M. Huang, J. Li, H.X. Shen, Peroxidase-based spectrophotometric methods for the determination of ascorbic acid, norepinephrine, epinephrine, dopamine and levodopa, Anal. Chim. Acta 357 (1997) 261–267.
[15] H. Beitollahia, I. Sheikhshoaie, Selective voltammetry determination of norepinephrine in the presence of acetaminophen and folic acid at a modified carbon nanotube paste electrode, J. Electroanal. Chem. 661 (2011) 336–342.
[16] H. Beitollahia, I. Sheikhshoaie, Electrocatalytic oxidation and determination of epinephrine in the presence of uric acid and folic acid at multiwalled carbon nanotubes/molybdenum(VI) complex modified carbon paste electrode, Anal. Meth. 3 (2011) 1810–1814.
[17] E. Molaakbari, A. Mostafavi, H. Beitollahi, R. Alizadeh, Synthesis of ZnO nanorods and their application in the construction of a nanostructure-based electrochemical sensor for determination of levodopa in the presence of carbidopa, Analyst 139 (2014) 4356–4364.
[18] H. Beitollahia, A. Mohadesi, S. Mohammadi, A. Akbari, Electrochemical behavior of a carbon paste electrode modified with 5-amino-3′,4′-dimethyl-biphenyl-2-ol/carbon nanotube and its application for simultaneous determination of isoproterenol, acetaminophen and N-acetylcysteine, Electrochim. Acta 68 (2012) 220–226.
[19] M. Dervisevic, E. Custiuc, E. Çevik, Z. Durmus, M. Şenel, A. Durmus, Electrochemical biosensor based on REGO Fe_3O_4 bionanocomposite interference for xanthine detection in fish sample, Food. Cont. 57 (2015) 402–410.
[20] T. Ruzgas, E. Csöregi, J. Emneus, L. Gorton, G. Marko-Varga, Peroxidase modified electrodes: fundamentals and application, Anal. Chim. Acta 330 (1996) 123–138.
[21] L. Wang, E. Wang, A novel hydrogen peroxide sensor based on horseradish peroxidase immobilized on colloidal Au modified ITO electrode, Electrochem. Commun. 6 (2004) 225–229.
[22] M. Giannoni, M. Parri, P. Chiarugi, EMT and oxidative stress: a bidirectional interplay affecting tumor malignancy, Antiox. Redox. Signal. 16 (2012) 1248–1263.
[23] C. Matsubara, N. Kawamoto, K. Takamura, Oxo[5,10,15, 20-tetra(4-pyridyl) porphyrinato]titanium (IV): an ultra-high sensitivity spectrophotometric reagent for hydrogen peroxide, Analyst 117 (1992) 1781–1784.
[24] K. Nakashima, K. Maki, S. Kawaguchi, S. Akiyama, Y. Tsukamoto, K. Imai, Peroxyoxalate chemiluminescence assay of hydrogen peroxide and glucose using 2,4,6,8-tetrathiomorpholinopyrimido[5,4-d]pyrimidine as a fluorescent component, Anal. Sci. 7 (1991) 709–713.
[25] E.C. Hurdis, J.H. Romeyn, Accuracy of determination of hydrogen peroxide by cerateoxidimetry, Anal. Chem. 26 (1954) 320–325.
[26] M. Dervisevic, E. Çevik, M. Şenel, Development of glucose biosensor based on reconstitution of glucose oxidase onto polymeric redox mediator coated pencil graphite electrodes, Enzym. Microb. Technol. 68 (2015) 69–76.
[27] B. Fang, S. Jiao, M. Li, Y. Qu, X. Jiang, Label-free electrochemical detection of DNA ferrocene-containing polythiophene and PNA probes on nanogold modified electrodes, Biosens. Bioelectron. 23 (2008) 1177–1179.
[29] N. Kuramoto, Y. Shishido, K. Nagai, Preparation of thermally responsive and electroactive poly(N-acryloylpyrrolidine-co-vinylferrocene), Macromol. Rapid Commun. 15 (1994) 441–444.
[30] S. Koide, K. Yokoyama, Electrochemical characterization of an enzyme electrode based on a ferrocene-containing redox polymer, J. Electroanal. Chem. 468 (1999) 193–201.
[31] G. Tanushree, S. Priyabrata, P.E.T. Anthony, A novel third generation uric acid biosensor using uricase electro-activated with ferrocene on a nafion coated glassy carbon electrode, Bioelectrochemistry 102 (2015) 1–9.
[32] P.E. Erden, Ş. Pekyardımcı, E. Kılıç, Amperometric enzyme electrode for xanthine determination with different mediators, Acta Chim. Slov. 59 (2012) 824–832.
[33] H. Katja, M. Marcus, S. Wolfgang, Fresen. Electron-transfer mechanisms in amperometric biosensors, J. Anal. Chem. 366 (2000) 560–568.
[34] J.F. Morin, From rods to sheets in a flash, Nat. Chem. 6 (2014) 463–464.
[35] H. Beitollahia, I. Sheikhshoaie, Electrochemical behavior of carbon nanotube/Mn(III) salen doped carbon paste electrode and its application for sensitive determination of N-acetylcysteine in the presence of folic acid, Int. J. Electrochem. Sci. 7 (2012) 7684–7698.
[36] Y. Wenrong, R.R. Kyle, P.R. Simon, T. Pall, J.G. Justin, B. Filip, Carbon nanomaterials in biosensors: should you use nanotubes or graphene? Angew. Chem. Int. Ed. 49 (2010) 2114–2138.
[37] H. Beitollahil, M. Mostafavi, Nanostructured based electrochemical sensor for simultaneous quantification and voltammetric studies of levodopa and carbidopa in pharmaceutical products and biological samples, Electroanalysis 26 (2014) 1090–1098.
[38] J.J. Gooding, F. Mearns, W.R. Yang, J.Q. Liu, Self assembled monolayers into the 21(st) century: recent advances and applications, Electroanalysis 15 (2003) 81–96.
[39] J.J. Gooding, Advances in interfacial design sensors: aryl diazonium salts for electrochemical biosensors and for modifying carbon and metal electrodes, Electroanalysis 20 (2008) 573–582.
[40] A. Heller, Electrical wiring of redox enzymes, Acc. Chem. Res. 23 (1990) 128–134.
[41] P.V. Bernhardt, Aust. Enzyme electrochemistry—biocatalysis on an electrode, J. Chem. 59 (2006) 233–256.
[42] J. Wang, Enzyme electrochemistry—biocatalysis on an electrode, Electroanalysis 19 (2007) 769–783.
[43] F. Patolsky, G.F. Zheng, C.M. Lieber, Nanowire-based biosensors, Anal. Chem. 78 (2006) 4260–4269.
[44] J. Wang, Electrochemical glucose biosensors, Chem. Rev. 108 (2008) 814–825.
[45] M. Portaccio, D. Di-Tuoro, F. Arduini, D. Moscone, M. Cammarota, D.G. Mita, M. Lepore, Laccase biosensor based on screen-printed electrode modified with thionine–carbon black composite, for bisphenol A detection, Electrochim. Acta 109 (2013) 340–347.
[46] X.H. Yang, Q. Yang, H. Yang, L. Wang, Y.Q. Chen, Performance and mechanism of screen-printed carbon paste electrode glucose biosensors based on functional carbon black, Chin. J. Anal. Chem. 35 (2007) 1751–1755.
[48] H.L. Joon, Y.P. Jae, M. Kyoungseon, J.C. Hyung, S.C. Suk, J.Y. Young, A novel organophosphorus hydrolase-based biosensor using mesoporous carbons and carbon black for the detection of organophosphate nerve agents, Biosens. Bioelectron. 25 (2010) 1566–1570.
[49] A. Celzard, J.F. Mareche, G. Furdin, Modelling of exfoliated graphite, Prog. Mater. Sci. 50 (2005) 93–179.
[50] H. Lei, G.B. Du, A. Pizzi, A. Celzard, Influence of nanoclay on urea-formaldehyde resins for wood adhesives and its model, J. Appl. Polym. Sci. 109 (2008) 2442–2451.
[51] I.M. Afanasov, D.V. Savchenko, S.G. Ionov, D.A. Rusakov, A.N. Seleznev, V.V. Avdeev, Thermal conductivity and mechanical properties of expanded graphite, Inorg. Mater. 45 (2009) 486–490.

[52] B. Felix, P. Vittoria, L.F. Sylvie, B. Annie, L. Peter, D. Laurent, S.M. Alfonso, An in situ small angle neutron scattering study of expanded graphite under a uniaxial stress, Carbon 57 (2013) 460–469.
[53] P. Francesco, P. Jürgen, Effect of the melt processing conditions on the conductive paths formation in thermoplastic polyurethane/expanded graphite (TPU/EG) composites, Compos. Sci. Technol. 80 (2013) 39–46.
[55] M. Florica, P. Aniela, R. Ciprian, M. Plamen, B. Adriana, B. Georgeta, P. Stephen, S. Joop, Voltammetric detection of urea on an Ag-modified zeolite-expanded graphite-epoxy composite electrode, Sensors 8 (2008) 5806–5819.
[56] F. Manea, A. Remes, C. Radovan, R. Pode, S. Picken, J. Schoonman, Simultaneous electrochemical determination of nitrate and nitrite in aqueous solution using Ag-doped zeolite-expanded graphite-epoxy electrode, Talanta 83 (2010) 66–71.
[57] K. Yong, C. Xiaohui, N. Junhua, Y. Shiping, W. Wenchang, L. Zhenyu, C. Zhidong, Palygorskite-expanded graphite electrodes for catalytic electro-oxidation of phenol, Appl. Clay Sci. 49 (2010) 64–68.
[59] M. Hongmin, W. Dan, C. Zhentao, L. Yan, Z. Yong, D. Bin, W. Qin, Graphene-based optical and electrochemical biosensors: a review, Anal. Lett. 46 (2013) 1–17.
[60] P.M. Ostrovsky, I.V. Gornyi, A.D. Mirlin, Electron transport in disordered grapheme, Phys. Rev. B 74 (2006) 235–443.
[61] M. Pumera, Graphene-based nanomaterials and their electrochemistry, Chem. Soc. Rev. 39 (2010) 4146–4157.
[62] X.S. Du, M. Xiao, Y.Z. Meng, A.S. Hay, Novel synthesis of conductive poly(arylene disulfide)/graphite composite, Synth. Met. 143 (2004) 129–132.
[63] T.L. Abdulazeez, Synthesis and utilisation of graphene for fabrication of electrochemical sensors, Talanta 131 (2015) 424–443.
[67] L. Farnaz, S. Zohreh, M. Pooria, A. Yatimah, S.A.M. Ninie, N. SAM, One-step hydrothermal green synthesis of silver nanoparticle-carbon nanotube reduced-graphene oxide composite and its application as hydrogen peroxide sensor, Sensors Actuators B 208 (2015) 389–398.
[68] C. Nan-Fu, H. Teng-Yi, Sensitivity and kinetic analysis of graphene oxide-based surface plasmon resonance biosensors, Sensors Actuators B 197 (2014) 35–42.
[69] F. Zengjie, L. Qianqian, G. Peiwei, L. Bin, W. Jinqing, Y.A. Shengrong, A new enzymatic immobilization carrier based on graphene capsule for hydrogen peroxide biosensors, Electrochim. Acta 151 (2015) 186–194.
[70] G.C. Bong, I. Jinkyu, S.K. Hoon, P. HoSeok, Flow-injection amperometric glucose biosensors based on graphene/nafion hybrid electrodes, Electrochim. Acta 56 (2011) 9721–9726.
[71] R. Alberto, C. Ignacio, B.G. Ana, Graphitization thermal treatment of carbon nanofibers, Carbon 59 (2013) 2–32.
[72] S. Iijima, Helical microtubules of graphitic carbon, Nature 354 (1991) 56–58.
[73] S. Arai, M. Endo, Carbon nanofiber composite powder prepared by electrodeposition, Electrochem. Commun. 5 (2003) 797–799.
[74] P. Werner, R. Verdejo, F. Wollecke, V. Altstadt, J.K.W. Sandler, M.S.P. Shaffer, Carbon nanofibers allow foaming of semicrystalline poly(ether ether ketone), Adv. Mater. 17 (2005) 2864–2869.
[75] J.S. Qiu, H.Z. Zhang, C.H. Liang, J.W. Li, Z.B. Zhao, Co/CNF catalysts tailored by controlling the deposition of metal colloids onto CNFs: preparation and catalytic properties, Chem. Eur. J. 12 (2006) 2147–2151.
[77] W. Lina, Z. Xueji, J. Huangxian, Amperometric glucose sensor based on catalytic reduction of dissolved oxygen at soluble carbon nanofiber, Biosens. Bioelectron. 23 (2007) 479–489.
[78] L. Xianbo, Z. Jianhua, L. Wu, L. Qing, L. Jinghong, Carbon nanofiber-based composites for the construction of mediator-free biosensors, Biosens. Bioelectron. 23 (2008) 1236–1243.
[79] R. Emily, P. Adaikkappan, T. Zuki, A.Z. David, P.M. Michael, J.A. Russell, H.L. Kendall, C. Bin, M. Meyyappan, E.K. Jessica, A carbon nanofiber based biosensor for simultaneous detection of dopamine and serotonin in the presence of ascorbic acid, Biosens. Bioelectron. 42 (2013) 434–438.
[80] L. Yang, W. Dawei, X. Lei, H. Haoqing, Y.A. Tianyan, A novel and simple route to prepare a Pt nanoparticle-loaded carbon nanofiber electrode for hydrogen peroxide sensing, Biosens. Bioelectron. 26 (2011) 4585–4590.
[81] J.S. Lopes, Perfect mismatch, Nat. Phys. 10 (2014) 709–711.
[82] A.P.F. Turner, Biosensors: sense and sensibility, Chem. Soc. Rev. 42 (2013) 3175–3648.
[83] J. Wang, Carbon-nanotube based electrochemical biosensors: a review, Electroanalysis 17 (2005) 7–14.
[84] R. Lei, Y. Dong, Enhanced enzyme activity through electron transfer between single-walled carbon nanotubes and horseradish peroxidase, Carbon 50 (2012) 1303–1310.
[86] I. Willner, R. Baron, B. Willner, Integrated nanoparticle biomolecule systems for biosensing and bioelectronics, Biosens. Bioelectron. 22 (2007) 1841–1852.
[87] R.S.V. Juan, D. Thomas, G. Oliver, S. Ivan, M. Andreas, J. Martin, A. Konstantin, R. Pascal, F. Roman, Controlled synthesis of single-chirality carbon nanotubes, Nature 512 (2014) 61–64.
[88] S.N. Lowrence, R.P. Deo, J. Wang, Comparison of the electrochemical reactivity of electrodes modified with carbon nanotubes from different sources, Electroanalysis 17 (2005) 65–72.
[89] A.P. Periasamy, Y.J. Chang, S.M. Chen, Amperometric glucose sensor based on glucose oxidase immobilized on gelatine multiwalled carbon nanotube modified glassy carbon electrode, Bioelectrochemistry 80 (2011) 114–120.
[90] D.R.J. Shobha, S. Ramaprabhu, S.N. Sriman, A thionine functionalized multiwalled carbon nanotube modified electrode for the determination of hydrogen peroxide, Carbon 45 (2007) 1340–1353.
[91] M. Dervisevic, E. Çevik, M. Şenel, Poly(GMA-co-VFc)/Fe3O4/cholesterol oxidase bionanocomposite based electrodes for amperometric cholesterol biosensor, Sens. Lett. 12 (2015) 1507–1512.
[92] W.S. Hummers, R.E. Offeman, Preparation of graphitic oxide, J. Am. Soc. 80 (1958) 1339–1339.
[93] S. Park, J. An, J.R. Potts, A. Velamakanni, S. Murali, R.S. Ruoff, Hydrazine-reduction of graphite- and graphene oxide, Carbon 49 (2011) 3019–3023.
[94] Z. Durmus, A. Durmus, H. Kavas, Synthesis and characterization of structural and magnetic properties of graphene/hard ferrite composites as microwave-absorbing material, J. Mater. Sci. 50 (2015) 1201–1213.
[95] C. Hou, W. Tang, C. Zhang, Y. Wang, N. Zhu, A novel and sensitive electrochemical sensor for bisphenol A determination based on carbon black supporting ferroferric oxide nanoparticles, Electrochim. Acta 144 (2014) 324–331.
[96] M. Dervisevic, E. Custiuc, E. Cevik, M. Şenel, Construction of novel xanthine biosensor by using polymeric mediator/MWCNT nanocomposite layer for fish freshness detection, Food Chem. 181 (2015) 277–283.
[97] A.S.E. Meibodi, S. Haghjoo, Amperometric urea biosensor based on covalently immobilized urease on an electrochemically polymerized film of polyaniline containing MWCNTs, Synth. Met. 194 (2014) 1–6.
[98] G. Yu, W. Wu, Q. Zhao, X. Wei, Q. Lu, Efficient immobilization of acetylcholinesterase onto amino functionalized carbon nanotubes for the fabrication of high sensitive organophosphorus pesticides biosensors, Biosensors Bioelectron. 68 (2015) 288–294.
[99] C. Lete, S. Lupu, B. Lakard, J.Y. Hihn, F.J. Campo, Multi-analyte determination of dopamine and catechol at single-walled carbon nanotubes – conducting polymer – tyrosinase based electrochemical biosensors, Electroanal. Chem. 744 (53) (2015) 53–61.
[100] T. Liu, H. Su, X. Qu, P. Ju, L. Cui, S. Ai, Acetylcholinesterase biosensor based on 3-carboxyphenylboronic acid/reduced graphene oxide–gold nanocomposites modified electrode for amperometric detection of organophosphorus and carbamate pesticides, Sensors Actuators B 160 (2011) 1255–1261.
[101] E.N. Navera, K. Soda, E. Tamiya, I. Karube, Development of acetylcholine sensor using carbon fiber (amperometric determination), Biosens. Bioelectron. 6 (1991) 675–680.